# Electronic Supplementary Information (ESI)

# Catalytic synergy of Au@$CeO_2$-rGO nanohybrids for the reductive transformation of antibiotics and dyes

*Kanchan Mishra,[a] Samjhana Pradhan,[a] Muhammad Saeed Akhtar,[a] Won-Guen Yang,[b] Sung Hong Kim[b] and Yong Rok Lee*[a]*

[a]School of Chemical Engineering, Yeungnam University, Gyeongsan 38541, Republic of Korea
*E-mail: yrlee@yu.ac.kr, Phone: 82-53-810-2529; Fax: 82-53-810-4631
[b]Analysis Research Division, Daegu Center, Korea Basic Science Institute, Daegu 41566, Republic of Korea

**Table of Contents**

## General remarks

## Materials and methods

Gold (III) chloride trihydrate ($HAuCl_4 \cdot 3H_2O$, 99.9%), cerium (III) chloride heptahydrate ($CeCl_3 \cdot 7H_2O$, 99%), graphite powder, potassium permanganate ($KMnO_4$), sucrose, ampicillin, ciprofloxacin, rhodamine B, and Congo red were obtained from Sigma-Aldrich. All the chemicals were used as received.

## Characterization of Au@$CeO_2$-rGO NHs

The optical properties of the Au@$CeO_2$-rGO NHs were studied using an Optizen 3220 (Double beam) UV-Vis spectrophotometer with a quartz cuvette and using distilled water as a reference. Powder X-ray diffraction (XRD) patterns were analyzed to determine the crystalline structure of the nanocomposites using PANalytical X'PertPRO MPD operating at 40 kV and 30 mA with Cu Kα as an X-ray source (λ = 1.5406 Å), scanning between 2θ = 10° and 2θ = 90° at a rate of 1.2°/min. The Raman spectra were measured using an XploRA Plus (HORIBA Scientific) with a TE air-cooled charge coupled device (CCD) detector to analyze the interfaces between components. The samples were excited with a YAG (Nd) laser at 532 nm; the spectral resolution was about 3 $cm^{-1}$, and the spectrum acquisition time was 100 s. The specific surface areas and pore sizes of the materials were analyzed from their adsorption-desorption isotherms using the Brunauer-Emmett-Teller (BET) and Barrett-Joyner-Halenda (BJH) models (Micrometrics). An Al Kα X-ray source was used to analyze the oxidation states of each element present in the core-shell nanocomposites using X-ray photoelectron spectroscopy (XPS, Thermo Scientific K-Alpha system). The ion source energy was between 100 V and 3 keV for the survey. The shape, size, and orientation of the core-shell nanocomposites were examined by field-emission transmission electron microscopy (FE-TEM, FEI Tecnai F20). The TEM samples were prepared by dipping a carbon-coated copper grid into the nanocomposite solution and allowing the solvent to evaporate at ambient temperature. The core-shell structure of the nanocomposites was analyzed using high-angle annular dark-field scanning TEM energy-dispersive X-ray spectroscopy (HAADF-STEM-EDS) at 200 kV with a point resolution of 0.24 nm, a Cs and Cc of 1.2 mm each, and a focal length of 1.7 mm, using a Genesis liquid nitrogen-cooled EDS detector with an ultrathin window. The thermal stability of the nanohybrids was measured by thermogravimetric analysis (TGA)

coupled with differential thermal calorimetry (DTA, SDT-Q600 V20.5 Build 15) from room temperature to 800 °C at a heating rate of 10 °C $min^{-1}$. The Raman spectra, BET, and BJH were recorded at the core research support center for natural products and medical materials of Yeungnam University.

**Characterization of transformed products**

All experiments were carried out in open air. Merck precoated silica gel plates (Art. 5554) with a fluorescent indicator were used for the analytical TLC. Flash column chromatography was performed using silica gel 9385 (Merck). The melting points are uncorrected and were determined using micro-cover glasses on a Fisher-Johns apparatus. The $^{1}H$ NMR spectra were recorded on a Varian-VNS (600 MHz) spectrometer using the solvent chemical shift at $d$ = 2.50 ppm for DMSO-$d_6$ or $d$ = 0.00 ppm for TMS as reference. The $^{13}C$ NMR spectra were recorded on a Varian-VNS (150 MHz) spectrometer using the solvent chemical shift at $d$ = 39.5 ppm for DMSO-$d_6$ as reference. Chemical shifts ($\delta$) are expressed in units of ppm and $J$ values are given in Hz. Multiplicities are abbreviated as follows; s = singlet, d = doublet, t = triplet, brs = broad singlet, dd = doublet of doublets, and m = multiplet. IR spectra were recorded on a FTIR (PerkinElmer, UATR Two) and GCMS was conducted in the temperature programming mode with SH-Rxi-5ms column (0.25 mm, 60 m; Rxi-5ms). The $^{1}H$ NMR, $^{13}C$ NMR and GC/MS spectra were recorded on VNS 600, 150 MHz and GCMS-QP2010 Ultra spectrometer, respectively at the core research support center for natural products and medical materials of Yeungnam University.

**General procedure for the reductive transformations of AMP, CIP, RhB, and CR on Au@$CeO_2$-rGO NHs**

The reductive transformation of AMP, CIP, CR and RhB was monitored by using UV-Vis, NMR ($^{1}H$ and $^{13}C$) NMR and GC MS analyses. Au@$CeO_2$-rGO NHs (2 mg) was added to a solution of AMP (0.025 mM in $H_2O$), CIP (0.025 mM in $H_2O$/DMSO), RhB (0.025 mM in $H_2O$/DMSO), or CR(0.025 mM in $H_2O$/DMSO), at room temperature. To the mixture, $NaBH_4$ (37.83 mg, 1.0 mmol) was added and the reaction mixture was then heated at 100°C for 1 h. After the complete transformation, the reaction mixture was extracted with ethyl acetate (20 mL x 2) and evaporated using a reduced pressure evaporator. The residue was purified by column chromatography on

silica gel to afford the reductive transformed products. The structure of the products were assigned by spectroscopic analysis.

**UV-Vis spectra of Au@$CeO_2$-rGO NHs**

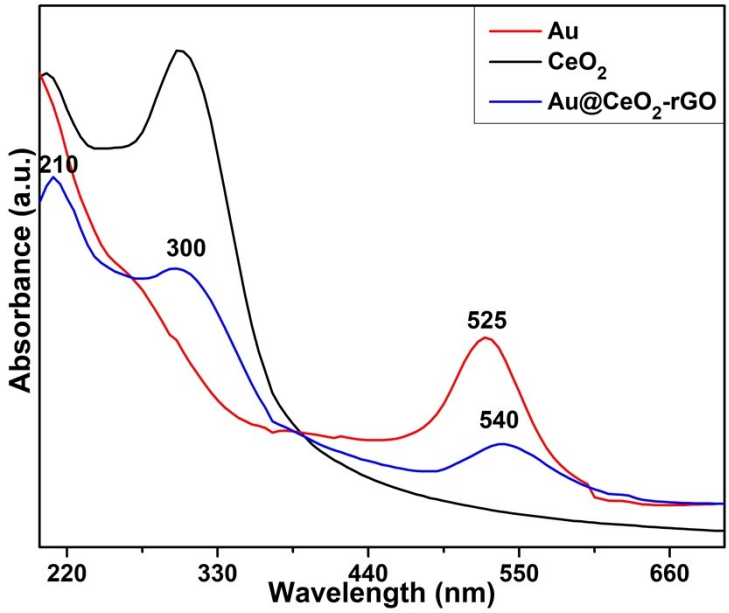


**Figure S1**. UV-Visible spectra of Au, $CeO_2$, and Au@$CeO_2$-rGO NHs

**EDS peaks of Au@$CeO_2$-rGO NHs**

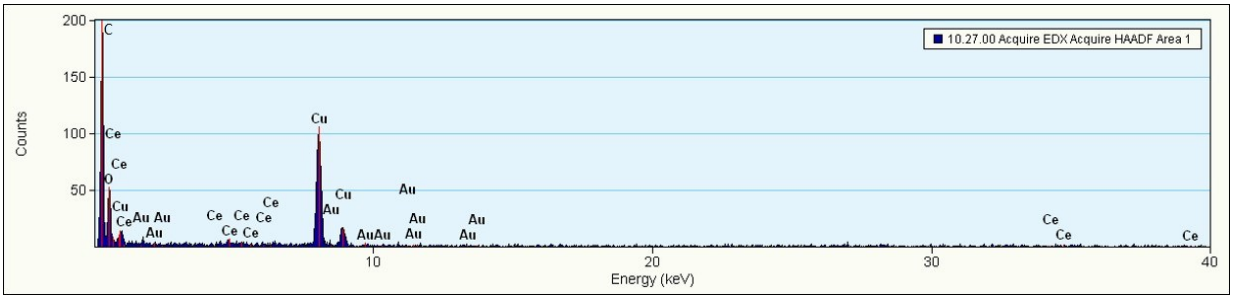


**Figure S2**. EDS peaks of Au@$CeO_2$-rGO NHs showing the characteristics peaks of C, O, Ce, and Au.

**TGA and DTA curves of the Au@$CeO_2$-rGO NHs**

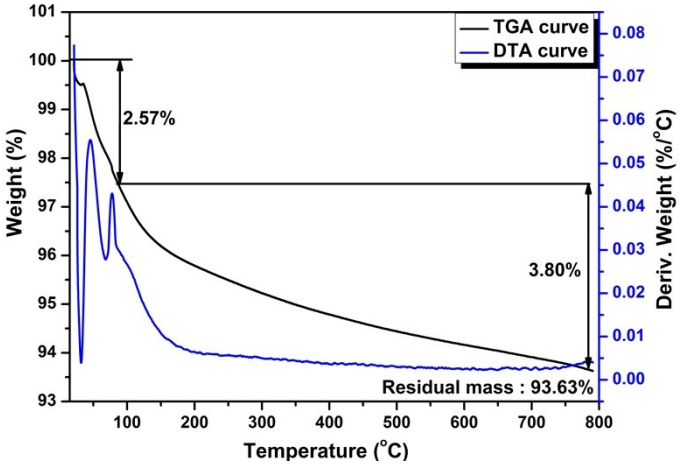


**Figure S3**. TGA and DTA curves of the Au@$CeO_2$-rGO NHs

**UV-Vis and FTIR spectra of transformed products**

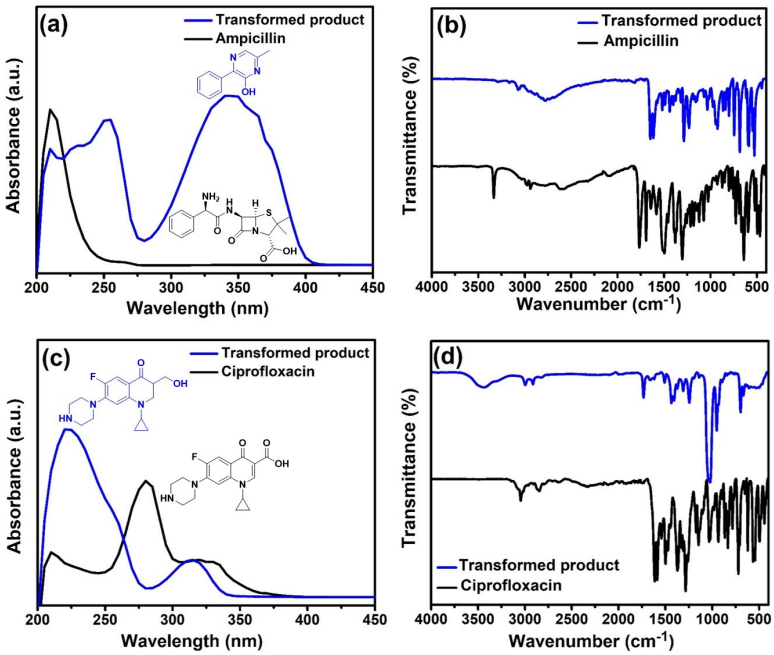


**Figure S4**. UV-Visible spectra of (a) Ampicillin and its transformed product, (c) Ciprofloxacin and its transformed product. FTIR spectra of (b) Ampicillin and its transformed product, (d) Ciprofloxacin and its transformed product.

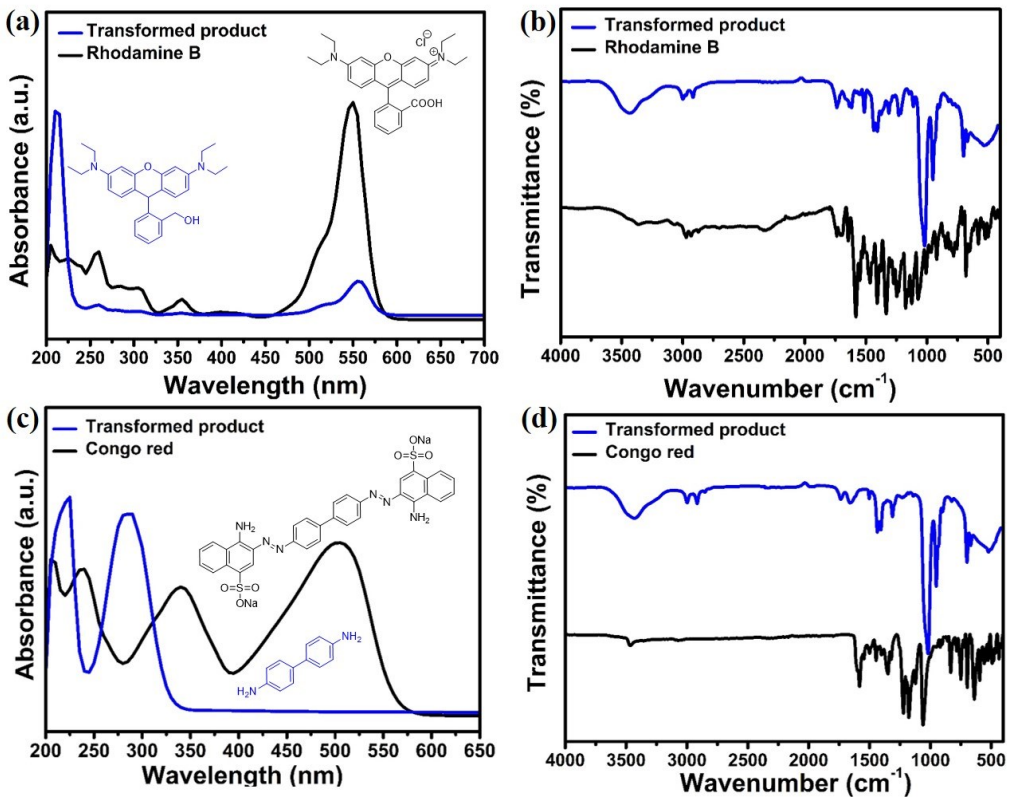


**Figure S5**. UV-Visible spectra of (a) Rhodamine B and its transformed product, (c) Congo red and its transformed product. FTIR spectra of (b) Rhodamine B and its transformed product, (d) Congo red and its transformed product.

**Characterization data of synthesized compounds**

**6-Methyl-3-phenylpyrazin-2-ol (2)**

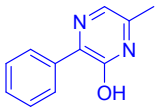

The title compound was prepared according to the general procedure. The product was obtained as a brown liquid. $^{1}$H NMR (600 MHz, DMSO-$d_6$) $\delta$ 12.43 (brs, 1H), 8.27 (dd, $J$ = 7.6, 1.7 Hz, 2H), 7.41 – 7.34 (m, 3H), 7.29 (s, 1H), 2.17 (s, 3H).; $^{13}$C NMR (150 MHz, DMSO-$d_6$) $\delta$ 156.1, 148.2, 138.0, 136.6, 129.3, 128.4, 128.1, 122.6, 16.01; IR (ATR) 2809, 1657, 1613, 1297, 1221, 971, 678, 526 cm$^{-1}$; GCMS *m/z* calcd for $C_{11}H_{10}N_2O$: 186. Found: 186.

**1-Cyclopropyl-6-fluoro-3-(hydroxymethyl)-7-(piperazin-1-yl)-2,3-dihydroquinolin-4(1*H*)-one (4)**

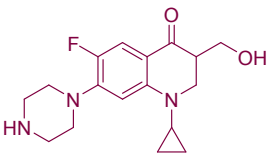

The title compound was prepared according to the general procedure. The product was obtained as a brown liquid. $^{1}$H NMR (600 MHz, DMSO-$d_6$ + $CDCl_3$) $\delta$ 7.25 (d, $J$ = 13.4 Hz, 1H), 6.63 (d, $J$ = 7.4 Hz, 1H), 6.15 (s, 1H), 3.44 (d, $J$ = 12.6 Hz, 2H), 3.39 (t, $J$ = 6.8 Hz, 2H), 3.00 (d, $J$ = 13.4 Hz, 2H), 2.92 (t, $J$ = 12.4 Hz, 2H), 2.64 – 2.56 (m, 3H), 2.46 (s, 1H), 2.43 (t, $J$ = 6.8 Hz, 2H), 2.30-2.27 (m, 1H), 0.84-0.81 (m, 2H), 0.62-0.61 (m, 2H); $^{13}$C NMR (150 MHz, DMSO-$d_6$ + $CDCl_3$) $\delta$ 190.6, 150.6, 147.7 ($J$ = 237.0 Hz), 144.8 ($J$ = 9.0 Hz), 112.9 ($J$ = 4.5 Hz), 112.8 ($J$ = 22.5 Hz), 102.7, 51.3, 50.9, 49.3, 47.6, 47.5, 40.4, 37.9, 31.8, 8.0; IR (ATR) 3450, 2993, 2918, 1743, 1428, 1254, 1015, 949, 689 cm$^{-1}$; GCMS *m/z* calcd for $C_{17}H_{22}FN_3O_2$: 319. Found: 319.

**(2-(3,6-Bis(diethylamino)-9*H*-xanthen-9-yl)phenyl)methanol (7)**

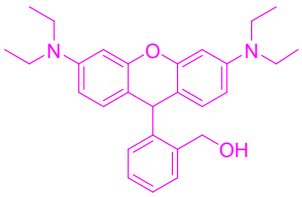

The title compound was prepared according to the general procedure. The product was obtained as a brown liquid. $^{1}$H NMR (600 MHz, DMSO-$d_6$) $\delta$ 7.34 (d, $J$ = 6.5 Hz, 1H), 7.10-7.08 (m, 2H), 6.94 (d, $J$ = 6.8 Hz, 1H), 6.69 (d, $J$ = 8.4 Hz, 2H), 6.27 (s, 3H), 6.25 (d, $J$ = 2.6 Hz, 1H), 5.34 (s, 1H), 5.25 (s, 1H), 4.55 (s, 2H), 3.25 (q, $J$ = 7.0 Hz, 8H), 1.04 (t, $J$ = 7.0 Hz, 12H); $^{13}$C NMR (150 MHz, DMSO-$d_6$) $\delta$ 151.7, 147.5, 138.9, 130.5, 130.4, 127.9, 127.7, 126.1, 111.4, 107.7, 98.2, 61.3, 44.10, 12.85; IR (ATR) 3450, 2998, 2929, 1728, 1625, 1511, 1433, 1224, 1024, 946, 712 cm$^{-1}$; GCMS *m/z* calcd for $C_{28}H_{34}N_2O_2$: 430. Found: 430.

**1,1'-Biphenyl-4,4'-diamine (10)**

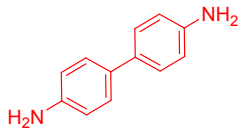

The title compound was prepared according to the general procedure. The product was obtained as a white solid. $^{1}$H NMR (600 MHz, DMSO-$d_6$) $\delta$ 7.22 (dd, $J$ = 8.6, 2.4 Hz, 4H), 6.62 (dd, $J$ = 8.6, 2.4 Hz, 4H), 5.48 (brs, 4H); $^{13}$C NMR (150 MHz, DMSO-$d_6$) $\delta$ 146.2, 129.6, 126.5, 115.3; IR (ATR) 3441, 3006, 2911, 1650, 1425, 1303, 1024, 946, 694 cm$^{-1}$; GCMS *m/z* calcd for $C_{12}H_{12}N_2$: 184. Found: 184.

**3,4-Diaminonaphthalene-1-sulfonic acid (11)**


The title compound was obtained according to the general procedure with slight modification. After the complete transformation of CR, the reaction mixture was extracted with ethyl acetate and water. The water extract was then treated with 0.1N HCl until yellow precipitate was formed. Then the yellow solid was filtered, washed with methanol and dried. The product was obtained as a brown solid. $^{1}$H NMR (600 MHz, DMSO-$d_6$) $\delta$ 8.70 (d, $J$ = 9.6 Hz, 1H), 8.05 (d, $J$ = 7.2 Hz, 1H), 7.78 (s, 1H), 7.43 – 7.38 (m, 2H); $^{13}$C NMR (150 MHz, DMSO-$d_6$) $\delta$ 139.0, 128.2, 128.1, 126.9, 125.2, 124.4, 121.9, 121.2, 117.5, 109.9; IR (ATR) 3488, 3318, 3186, 1639, 1406, 1352, 992, 944, 808, 602, 524 cm$^{-1}$; GCMS *m/z* calcd for $C_{10}H_{10}N_2O_3S$: 238. Found: 238.

## $^{1}$H NMR and $^{13}$C NMR spectra of synthesized compounds

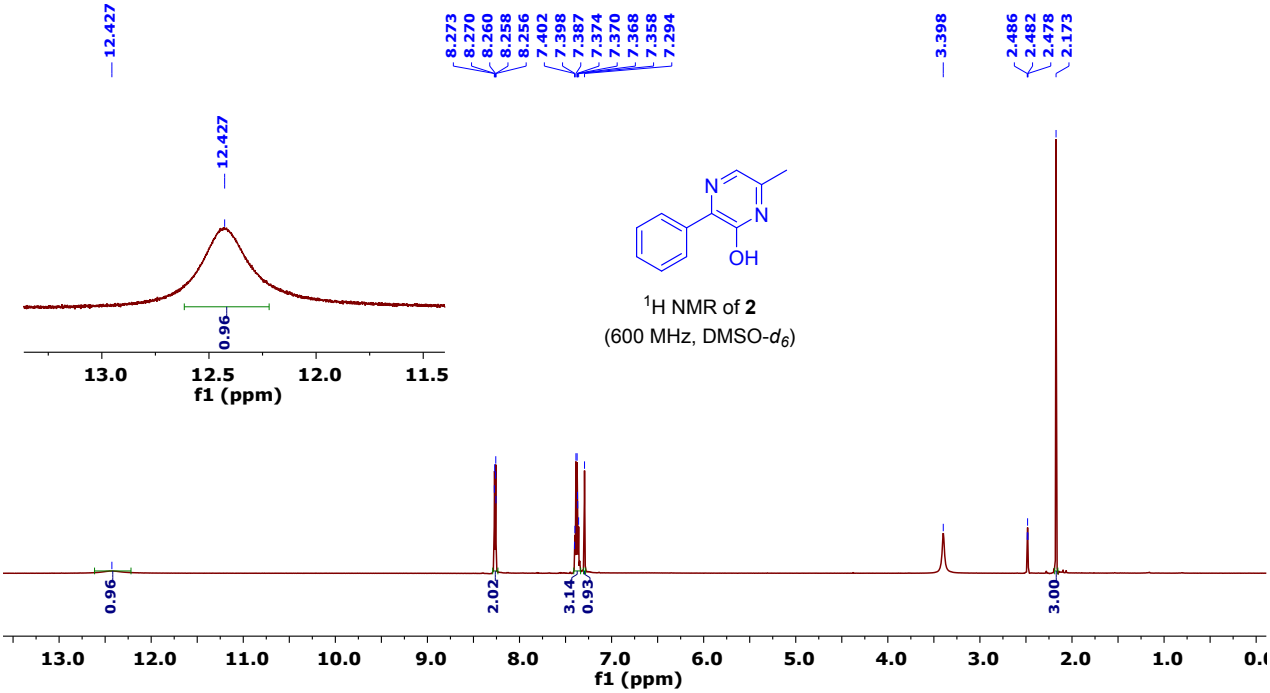


$^{1}$H NMR of **2**
(600 MHz, DMSO-$d_6$)

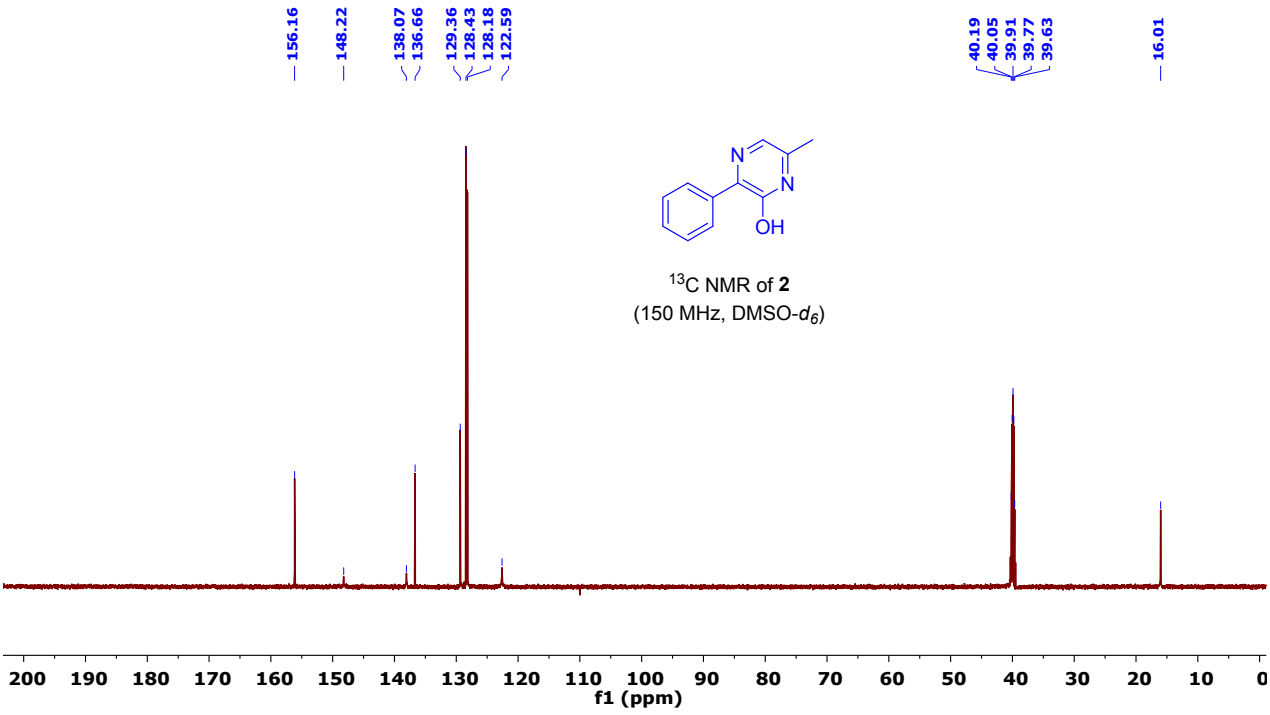


$^{13}$C NMR of **2**
(150 MHz, DMSO-$d_6$)

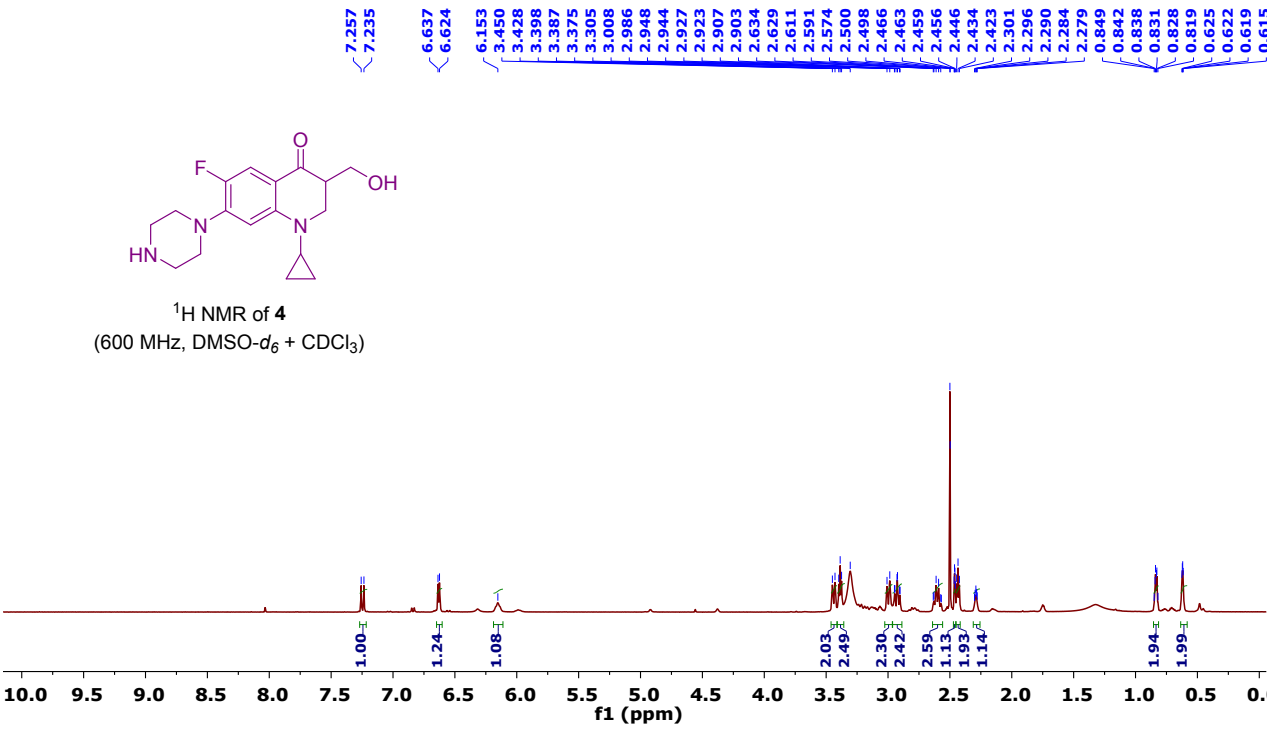


$^{1}$H NMR of **4**
(600 MHz, DMSO-$d_6$ + $CDCl_3$)

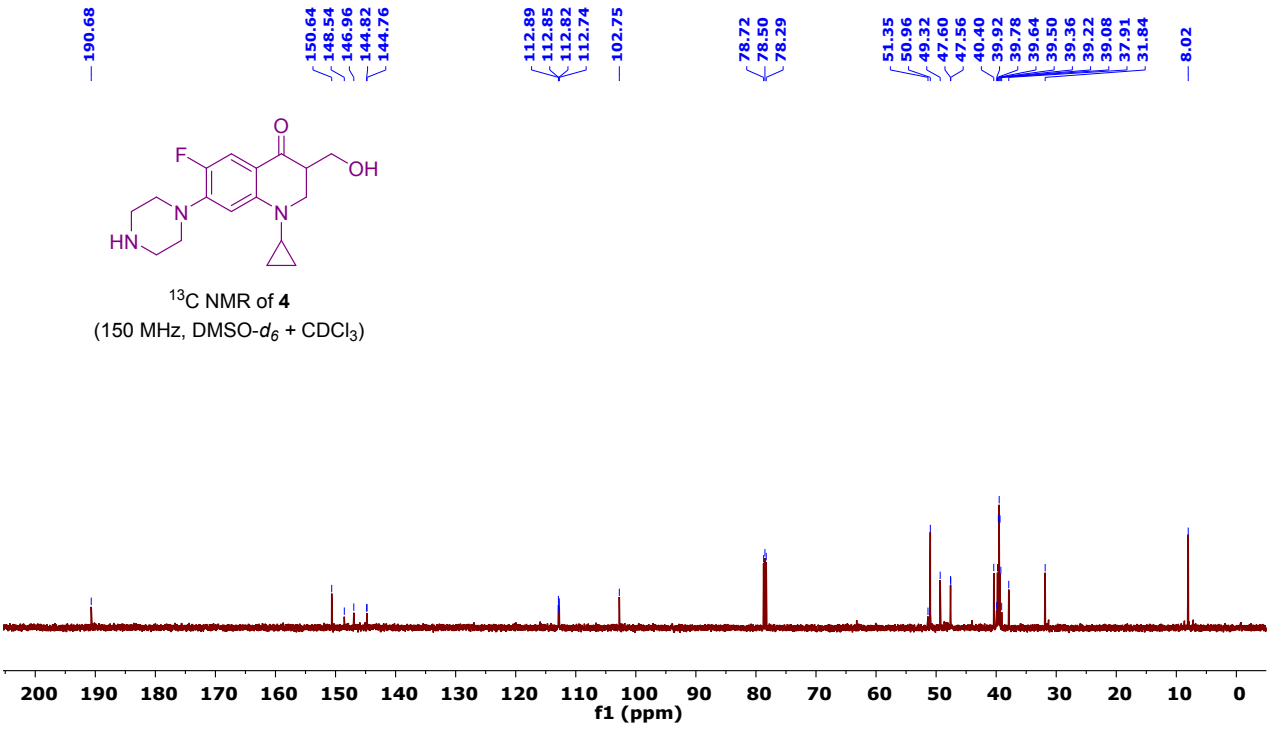


$^{13}$C NMR of **4**
(150 MHz, DMSO-$d_6$ + $CDCl_3$)

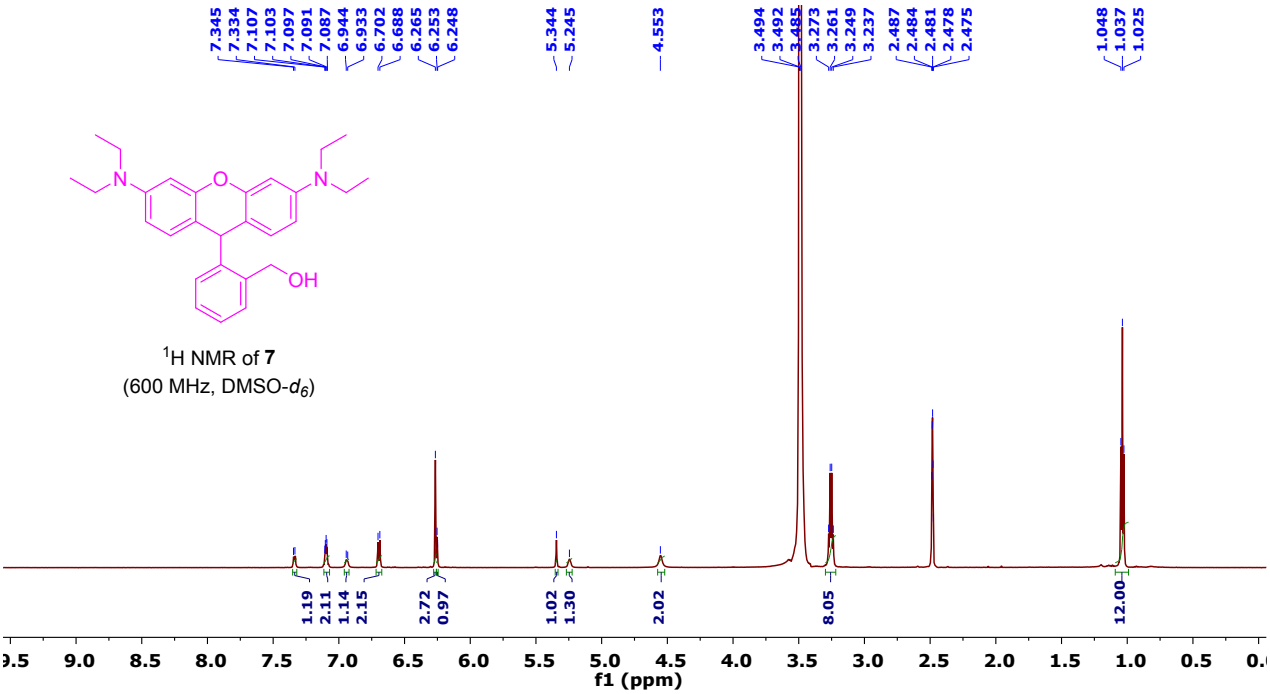


$^{1}$H NMR of **7**
(600 MHz, DMSO-$d_6$)

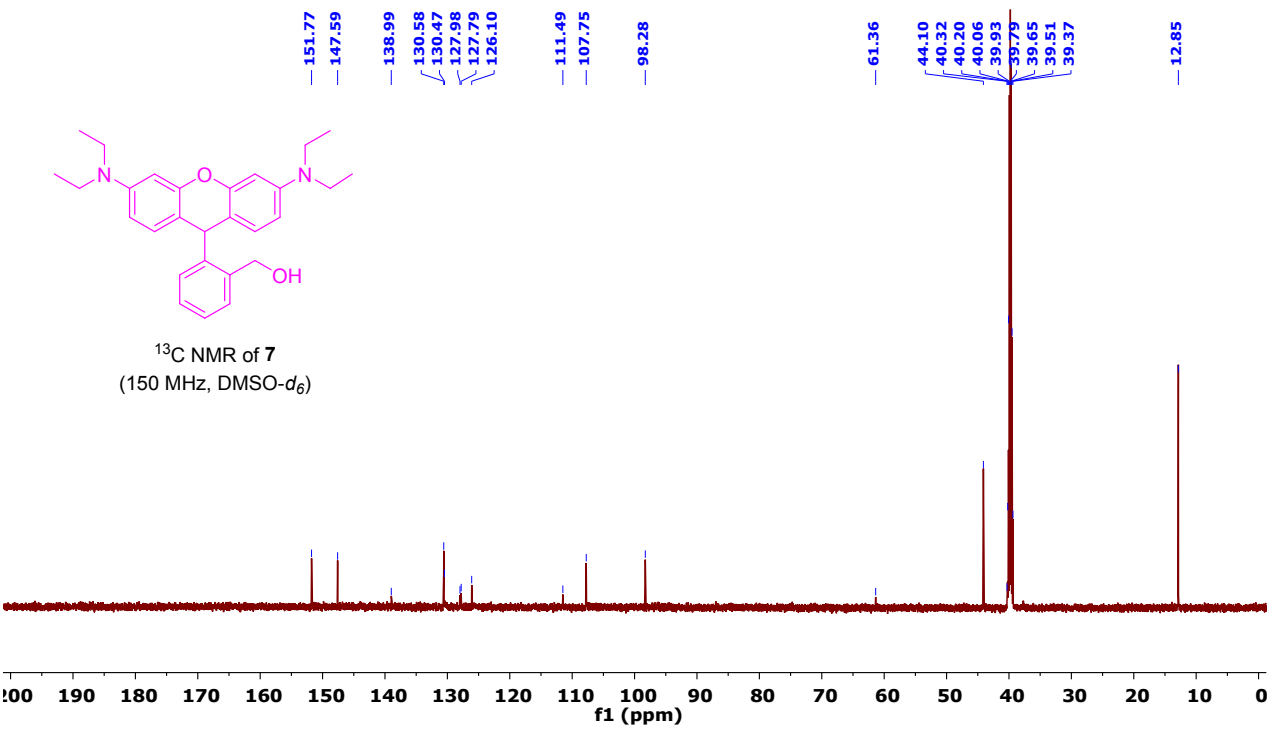


$^{13}$C NMR of **7**
(150 MHz, DMSO-$d_6$)

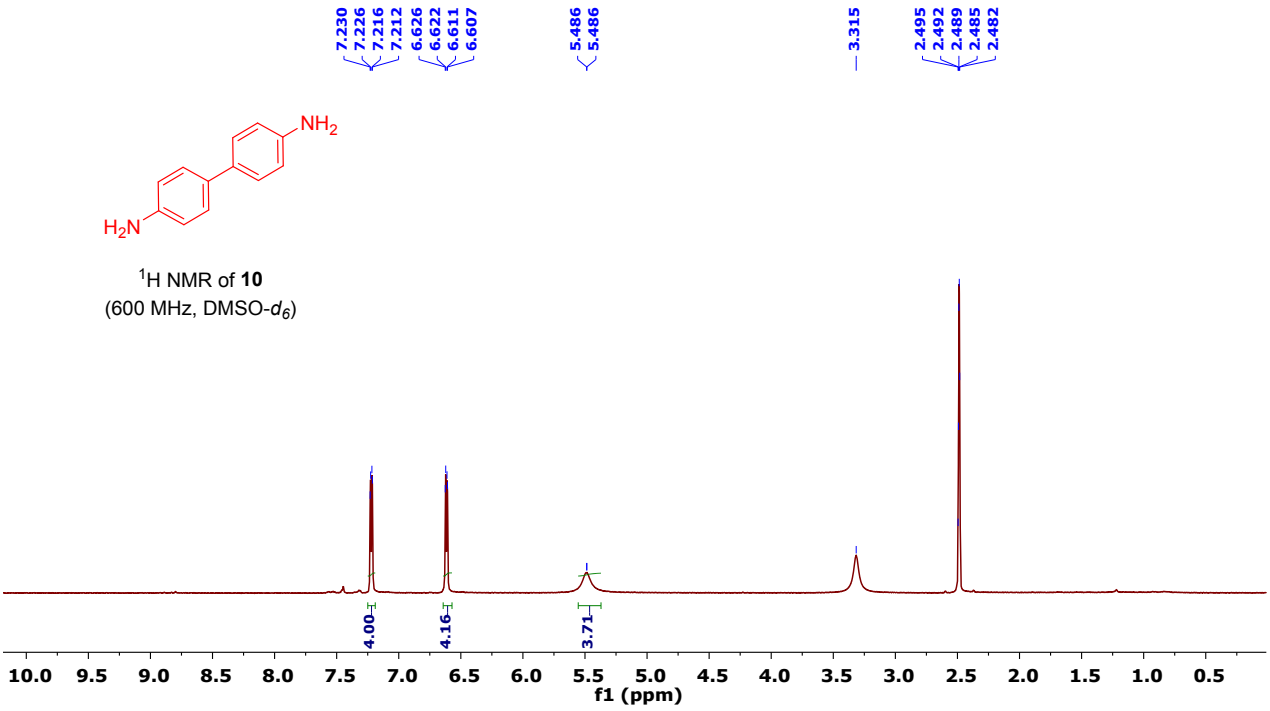


$^{1}$H NMR of **10**
(600 MHz, DMSO-$d_6$)

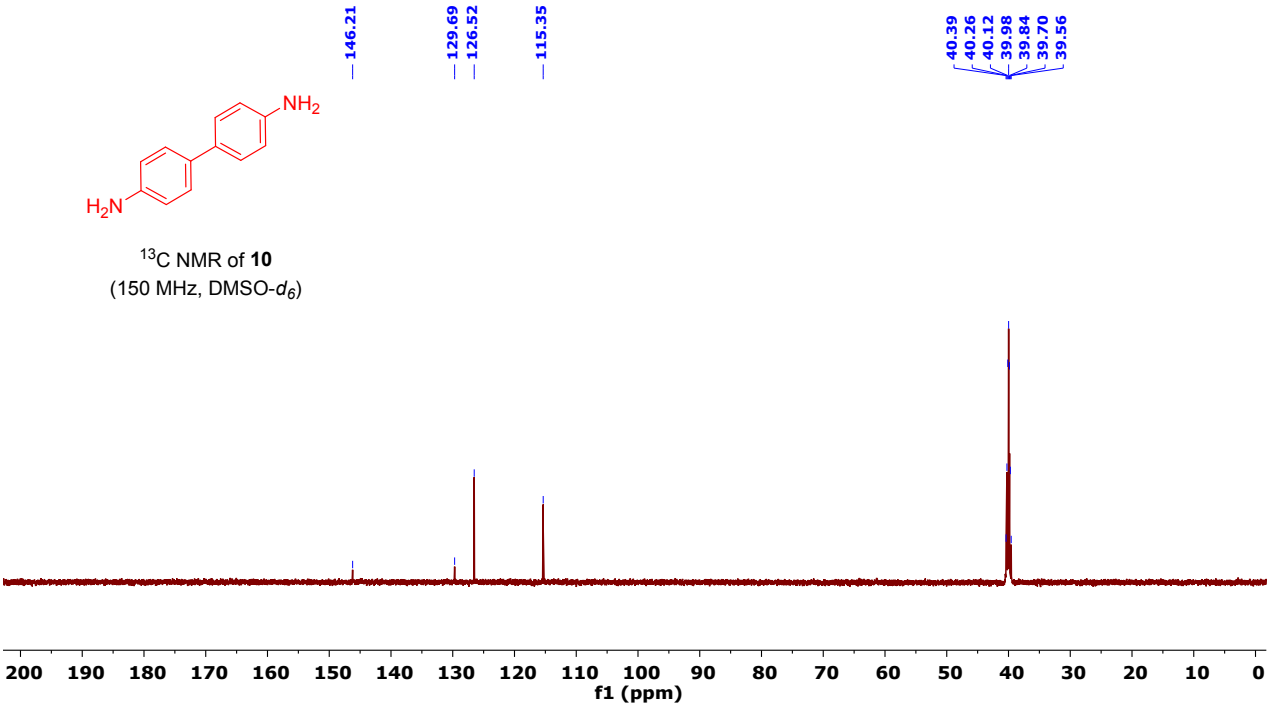


$^{13}$C NMR of **10**
(150 MHz, DMSO-$d_6$)

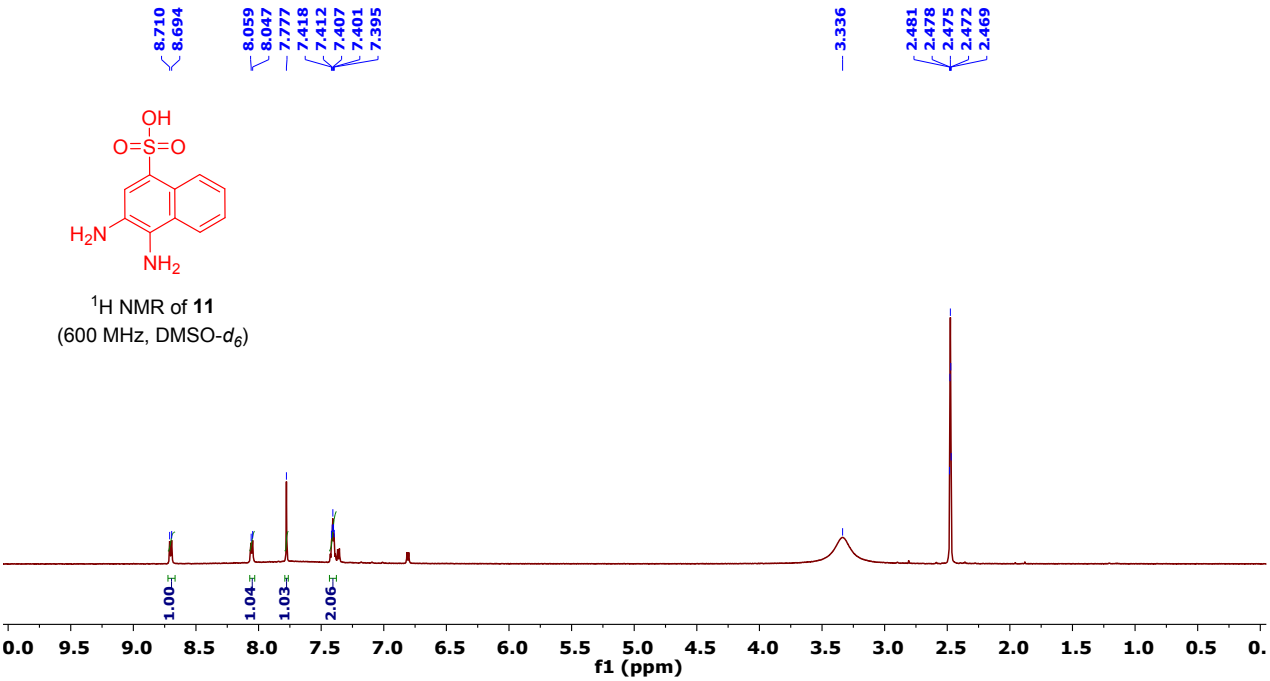


$^{1}$H NMR of **11**
(600 MHz, DMSO-$d_6$)

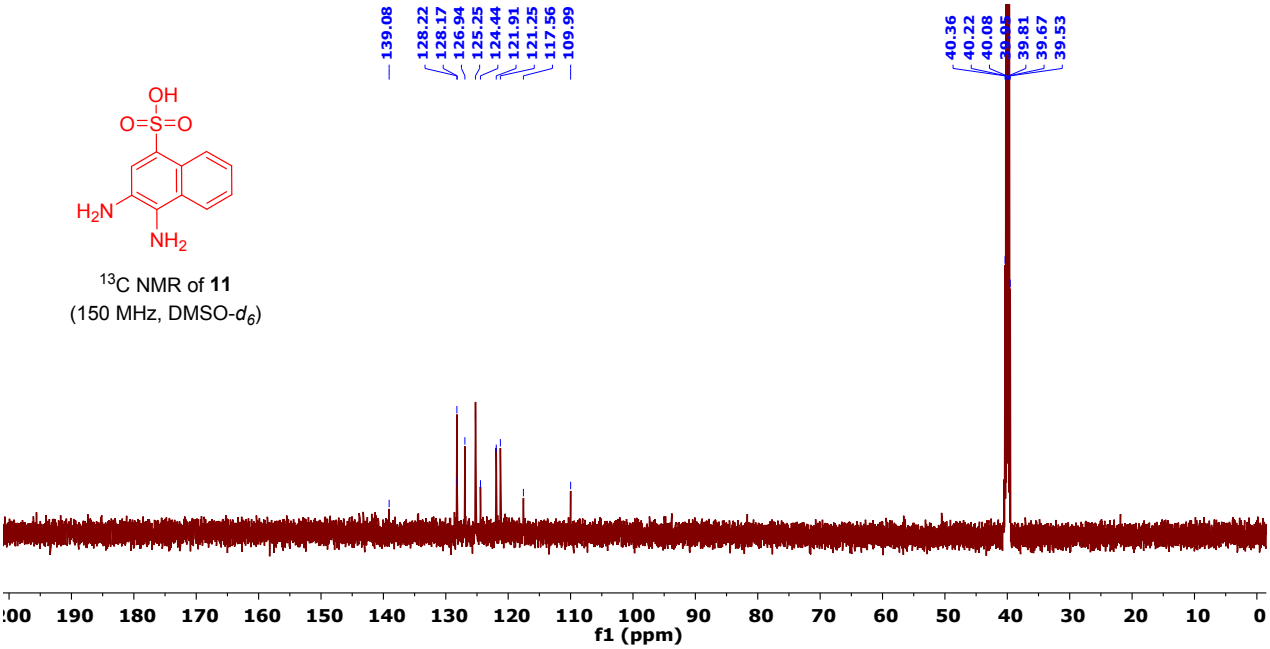


$^{13}$C NMR of **11**
(150 MHz, DMSO-$d_6$)

## GC-MS spectra of transformed products

**GC MS spectra of transformed product of AMP**

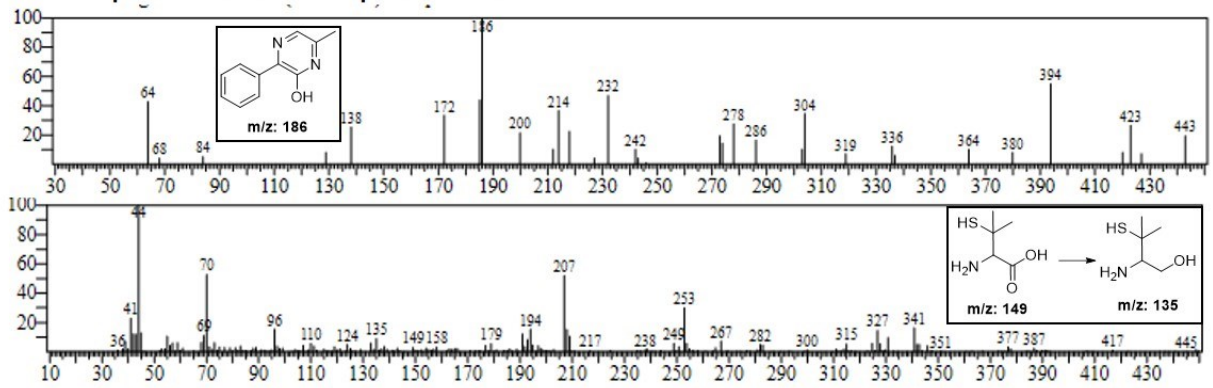


**GC MS spectra of transformed product of CIP**

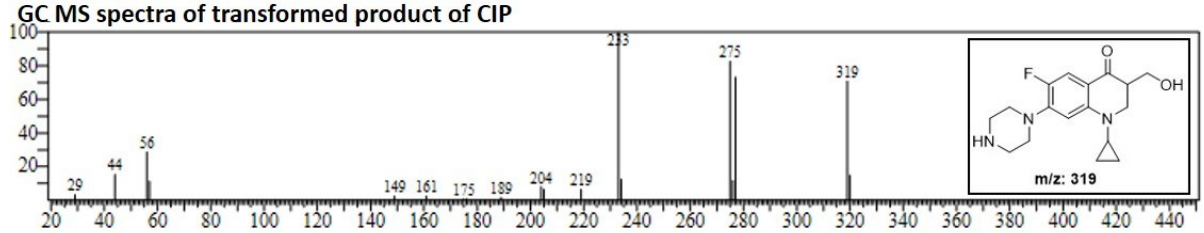


**GC MS spectra of transformed product of RhB**

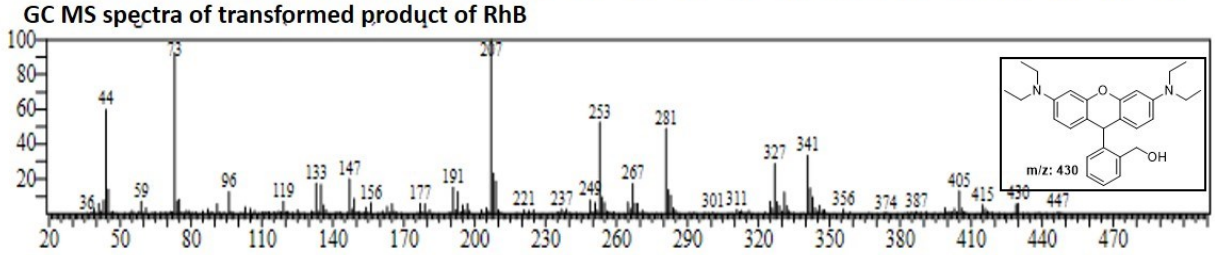


**GC MS spectra of transformed product of CR**

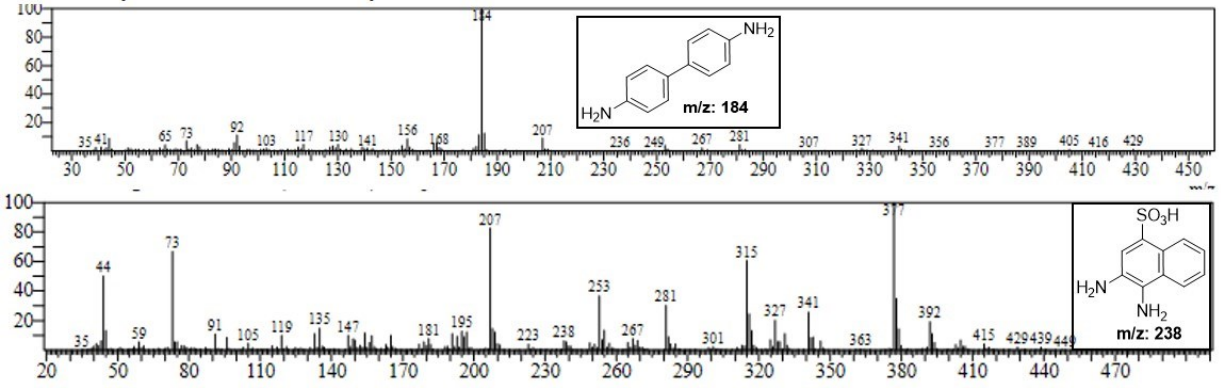

**Antibacterial activity elimination of AMP and CIP**

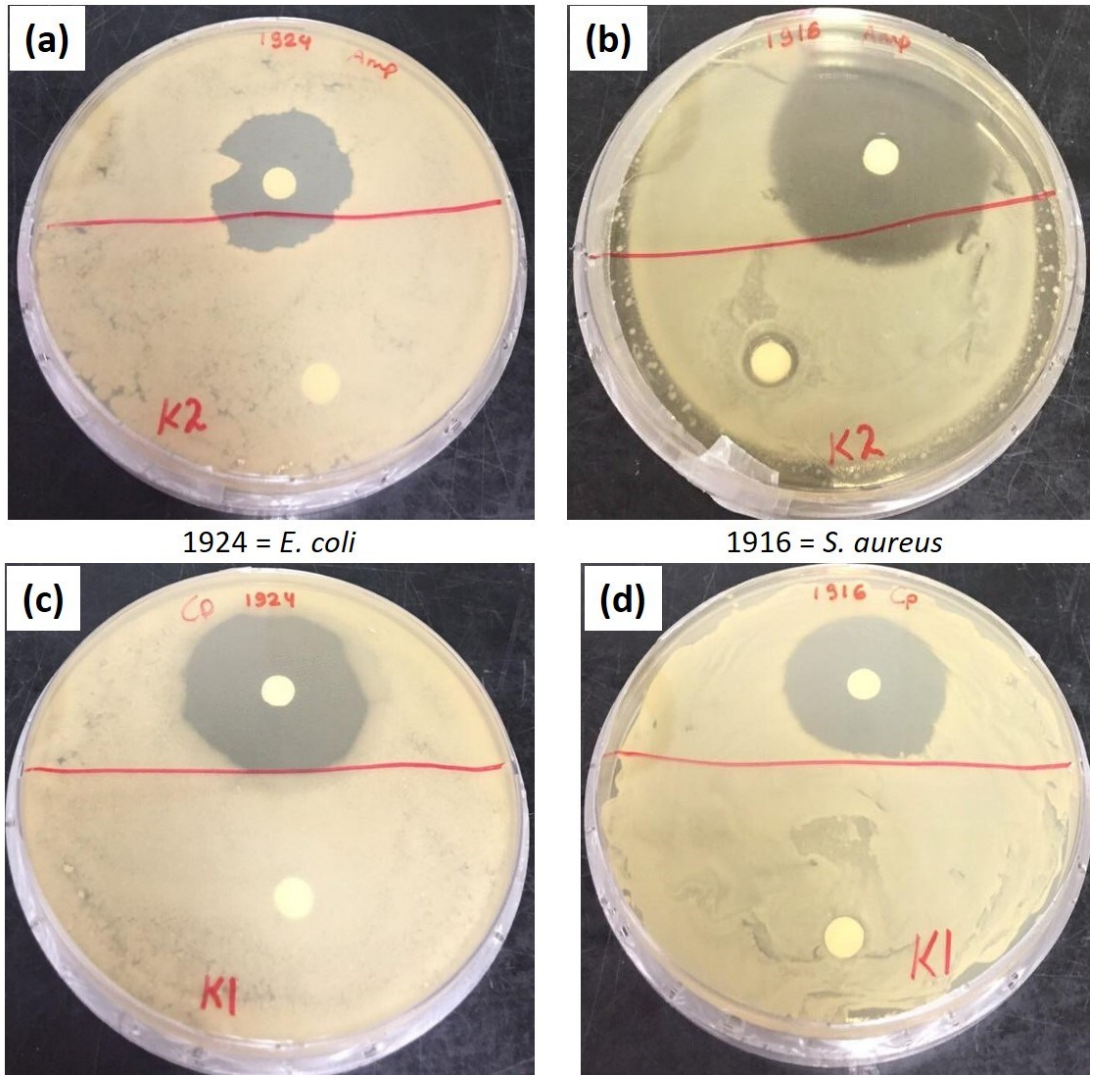


**Figure S6**. Zone of inhibition of AMP while using (a) *E. Coli* (1924), and (b) *S. aureus* (1916); K2 = transformed product **2**, which did not show any antibacterial activity in both cases. Zone of inhibition of CIP while using (c) *E. Coli* (1924), and (d) *S. aureus* (1916); K1 = transformed product **4**, which did not show any antibacterial activity in both cases.